Available online at www.derpharmachemica.com

Scholars Research Library

Der Pharma Chemica, 2012, 4 (3): 1145-1152
(http://derpharmachemica.com/archive.html)

ISSN 0975-413X
CODEN (USA): PCHHAX

Comparative Molecular Field Analysis Study on 2-(Substituted)-N-(5-Aryl-1,3,4-Thiadiazol-2-yl)Acetamide Derivatives for Spontaneous Motor Activity

Sanmati K. Jain[*1] and Pradeep Mishra[2]

*[*1]SLT Institute of Pharmaceutical Sciences, Guru Ghasidas Vishwavidyalaya, Bilaspur, India*
[2]GLA Institute of Pharmaceutical Research (GLAIPR), PO Chaumuha, Mathura, India

---

ABSTRACT

Three-dimensional quantitative structure activity relationship (3D-QSAR) study using comparative molecular field analysis (CoMFA) was performed on 2-(Substituted)-N-(5-aryl-1,3,4-thiadiazol-2-yl)acetamide derivatives for spontaneous motor activity. This study was performed using 42 compounds, in which the CoMFA model was developed using a training set of 36 compounds. Six compounds (selected randomly served as a test set), which were not used in model generation, were used to validate the CoMFA model. CoMFA derived QSAR model shows a good conventional squared correlation coefficient r^2 and cross validated correlation coefficient r^2cv 0.889 and 0.714 respectively. In this analysis steric and electrostatic field contribute to the QSAR equation by 83.3% and 16.7% respectively, suggesting that variation in biological activity of the compounds is dominated by differences in steric (van der Waals) interactions. To visualize the CoMFA steric and electrostatic field from PLS analysis, contour maps are plotted as percentage contribution to the QSAR equation and are associated with the differences in biological activity.

Keywords: 3D-QSAR, CoMFA, 2-(Substituted)-N-(5-aryl-1,3,4-thiadiazol-2-yl)acetamides, Spontaneous Motor Activity.

INTRODUCTION

Comparative Molecular Field Analysis (CoMFA) is a three-dimensional quantitative structure activity relationship (3D-QSAR) approach, introduced in 1988 by Cramer [1,2]. From the very first formulation of a lattice model to compare molecules by aligning them with a putative pharmacophore and by mapping their surrounding fields to a three-dimensional grid, CoMFA approach was an application of the dynamic lattice oriented molecular modeling system (DYLOMMS), as it was called till 1987. CoMFA is by far the most often employed receptor- independent (RI) 3D-QSAR approach, reflecting a novel, conceptually satisfying scientific approach reduced to practice as a well-written and versatile software package. In this method a relationship is established between the biological activities of a set of compounds and their steric and electrostatic properties [3-6]. 1,3,4-thiadiazole is a versatile pharmacophore and the compounds having this nucleus is responsible for a broad spectrum of biological activities, i.e. carbonic anhydrase inhibitory [7-16], antimicrobial [17-21], anti-inflammatory [22-24], anticancer [25,26], antitubercular [27-30], anti H-pylori [31], antidiabetic [32], anti-HIV [33], antileishmanial [34], etc. For establishing relationship between structure and biological activities of the synthesized compounds [35-37] quantitatively, three-dimensional quantitative structure activity relationship (CoMFA) study was carried out.

Table-1: Structure and biological activities of training set molecules (36)

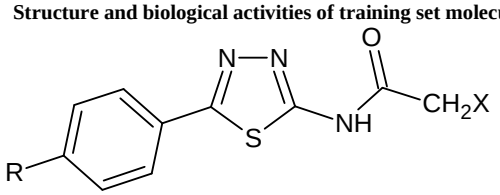

Compound No.	R	X	AA*	Mol. Wt.	BA**	log BA
1	H	Di-*n*-propyl amino	69.81	318.44	0.2223	-0.65
2	H	Di-*iso*-propyl amino	61.49	318.44	0.1958	-0.71
3	H	Di-*n*-butylamino	78.63	346.49	0.2724	-0.56
4	H	Morpholino	54.65	304.37	0.1663	-0.78
5	H	4-Methyl piperidino	59.33	316.42	0.1877	-0.73
6	H	Piperidino	67.5	302.42	0.2041	-0.69
7	H	N-Methyl piperazino	72.64	317.41	0.2306	-0.64
8	H	Pyrrolidino	58.15	288.37	0.1677	-0.78
9	H	Dicyclohexyl amino	65.22	398.57	0.2599	-0.59
10	H	Pyrrolidin-2-one-1-yl	52.64	302.35	0.1591	-0.80
11	CH_3O	Di-*n*-propyl amino	80.19	348.46	0.2794	-0.55
12	CH_3O	Di-*iso*-propyl amino	80.73	348.46	0.2813	-0.55
13	CH_3O	*n*-Butyl methyl amino	75.00	334.44	0.2508	-0.60
14	CH_3O	Di-*iso*-butyl amino	63.48	376.52	0.2390	-0.62
15	CH_3O	Morpholino	68.51	334.39	0.2290	-0.64
16	CH_3O	4-Methyl piperidino	78.42	346.45	0.2717	-0.57
17	CH_3O	Piperidino	86.79	332.42	0.2885	-0.54
18	CH_3O	N-Methyl piperazino	84.28	347.44	0.2928	-0.53
19	CH_3O	Pyrrolidino	61.29	318.39	0.1951	-0.71
20	CH_3O	Dicyclohexyl amino	82.02	428.59	0.3515	-0.45
21	CH_3O	Pyrrolidin-2-one-1-yl	73.63	332.38	0.2448	-0.61
22	CH_3	Di-*n*-propyl amino	85.13	332.46	0.2830	-0.55
23	CH_3	Di-*n*-butylamino	88.54	360.52	0.3192	-0.50
24	CH_3	Di-*iso*-butyl amino	69.46	360.52	0.2504	-0.60
25	CH_3	4-Methyl piperidino	81.78	330.45	0.2702	-0.57
26	CH_3	Piperidino	87.53	316.42	0.2769	-0.56
27	CH_3	N-Methyl piperazino	85.75	331.44	0.2842	-0.55
28	CH_3	Pyrrolidino	82.03	302.39	0.2480	-0.60
29	CH_3	Dicyclohexyl amino	83.65	412.59	0.3451	-0.46
30	CH_3	Pyrrolidin-2-one-1-yl	76.52	316.38	0.2421	-0.62
31	Cl	Di-*n*-propyl amino	77.20	352.88	0.2724	-0.56
32	Cl	Di-*iso*-propyl amino	72.70	352.88	0.2565	-0.59
33	Cl	Di-*n*-butylamino	83.88	380.94	0.3195	-0.56
34	Cl	Piperidino	57.63	336.84	0.1941	-0.71
35	Cl	N-Methyl piperazino	61.5	351.85	0.2164	-0.66
36	Cl	Dicyclohexyl amino	48.54	433.01	0.2102	-0.68

** = Percent spontaneous motor activity at 100 mg/kg body weight orally; ** = Percent spontaneous motor activity per micromole of drug per kilogram of body weight.*

MATERIALS AND METHODS

Data Set: A dataset of 42 molecules synthesized [35-37] earlier [2-(Substituted)-N-(5-aryl-1,3,4-thiadiazol-2-yl)acetamide derivatives] having spontaneous motor activity using Actophometer has been taken for the present study (Table-1). Selected data set, their biological activities are shown in Table-1 and 2 forming the training and test set respectively. For CoMFA studiy, logarithmic value of biological activity (logBA) was taken, while BA is calculated using the following formulae [38]. BA is expressed as percent spontaneous motor activity per micro mole of drug per kilo gram of body weight.

BA = % Spontaneous Motor Activity × Mol. Wt. / dose (g) × 10^6

Table-2: Structure and biological activities of test set molecules (06)

Compound No	R	X	AA*	Mol. Wt.	BA**	log(BA)
1	H	Di-*iso*-butyl amino	58.17	346.49	0.2015	-0.70
2	CH_3O-	Di-*n*-butyl amino	82.66	376.52	0.3112	-0.51
3	CH_3	Di-*iso*-propyl amino	83.48	332.46	0.2775	-0.56
4	CH_3	*n*-Butyl methyl amino	77.27	318.44	0.2460	-0.61
5	CH_3	Morpholino	75.43	318.39	0.2402	-0.62
6	Cl	*n*-Butyl methyl amino	85.71	338.86	0.2904	-0.54

** = Percent spontaneous motor activity at 100 mg/kg body weight orally;*
*** = Percent spontaneous motor activity per micromole of drug per kilogram of body weight.*

Molecular Modeling: Molecular Modeling and CoMFA studies were performed on Silicon Graphics Octane computer using molecular modeling package SYBYL 6.5 using the standard TRIPOS force field. Structural manipulations were performed with molecular modeling package SYBYL 6.5 using the standard TRIPOS force field. Partial atomic charges of ligands were calculated using within MOPAC. The structures were then optimized by energy minimization using the Powell algorithm to a final root mean square gradient of 0.05 kcal / mol.

Alignment: The alignment, i.e. molecular conformation and orientation, is one of the sensitive inputs for CoMFA. One of the most active compounds used as a reference compound. The compounds were fitted to the active analogue compound.

GRID Size: Once the molecules are aligned a grid or lattice is established which surrounds the set of analogs in potential receptor space. Current CoMFA studies seldom use grid resolution less then 1 A^o and, most often, 2 A^o. The choice of grid resolution represents a compromise between computational practicality and detailing of the fields. If the grid resolution is too small, the number of field–points (cells) becomes too large to perform a timely analysis. Moreover spatial information on field preference can be lost, through a 'smearing out' effect, if the cells become too small. The grid resolution in the 1 to 2 A^o range corresponds to, at best, differentiating single carbon-carbon (1.54 A^o) from one another.

CoMFA Interaction Energy: The steric and electrostatic (potential fields) energies were calculated at each lattice intersection of a regularly spaced grid box. The lattice spacing was set a value of 2.0 A^o. CoMFA region was defined automatically which extends the lattice walls beyond the dimensions of each structures by 4.0 A^o in all directions. The Lennard-Jones Potential and coloumbic term which represent, respectively steric and electrostatic fields, were calculated using the TRIPOS force fields.

An sp^3 carbon atom with a van der Waals radius of 1.52 A^o and a +1.0 charge served as the probe atom to calculate steric and electrostatic fields. The default value of 30.0 kcal/mol was used as the maximum electrostatic and steric energy cutoff.

Partial least squares (PLS) and Cross-validation in CoMFA: The last step in a CoMFA is a partial least square analysis to determine the minimal set of grid points which is necessary to explain the biological activities of the compounds. Partial least–squares is an iterative procedure that applies two criteria to produce its solution. First, to extract a new component, the criterion is to maximize the degree of commonality between all of the structural parameter columns (independent variable) collectively and the experimental data (dependent variable). Second, in the evaluation phase of a PLS iteration, the criterion for acceptance of the principal component just generated is an improvement in the ability to predict, not to reproduce, the dependent variable.

The technique used in PLS to assess the predictive ability of a QSAR is cross-validation [39]. Cross-validation is based on the idea that the best way to assess predictive performance is to predict. When cross-validating, one pretends that one or more of the unknown experimental value is, infect, unknown. The analysis being cross-validated is repeated, excluding the temporarily 'unknown' compounds and then using the resulting equation to predict the experimental measurement of the omitted compound(s). The cross-validation cycle is repeated until each compound has been excluded and predicted exactly once. The results of cross-validation are the sum of the squared prediction errors, sometimes called the predicted residual sum of squares (PRESS). For evaluation of the overall analysis, the PRESS is commonly expressed as a cross–validated correlation coefficient r^2 or xv-r^2 value.

RESULTS AND DISCUSSSION

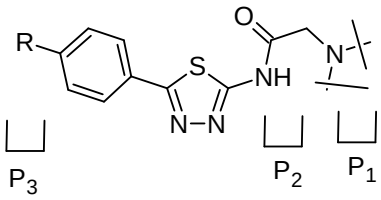

Figure-1

Table-3: Summary of CoMFA results

r^2 conventional	0.889
Standard error of estimate	0.030
F value	62.098
P value	0.000
r^2 cross-validated	0.714
Standard error of predictions	0.049
No. of components	4
Steric contribution	0.833
Electrostatic contribution	0.167

** Results from leave one out (LOO) cross validation analysis using four components.*

Table-4: Data from PLS Cross-validated analysis (For Training Set)

Compound	Actual log (BA)	Calculated log (BA)	Residual
01	-0.65	-0.65	0.00
02	-0.71	-0.69	-0.02
03	-0.56	-0.60	0.04
04	-0.78	-0.76	-0.02
05	-0.73	-0.70	-0.03
06	-0.69	-0.71	+0.02
07	-0.64	-0.69	+0.05
08	-0.78	-0.79	+0.01
09	-0.59	-0.58	-0.01
10	-0.80	-0.75	-0.05
11	-0.55	-0.55	0.00
12	-0.55	-0.55	0.00
13	-0.60	-0.60	0.00
14	-0.62	-0.62	0.00
15	-0.64	-0.64	0.00
16	-0.57	-0.57	0.00
17	-0.54	-0.59	0.05
18	-0.53	-0.56	0.03
19	-0.71	-0.66	-0.05
20	-0.45	-0.46	0.01
21	-0.61	-0.62	0.01
22	-0.55	-0.51	-0.04
23	-0.50	-0.46	-0.04
24	-0.60	-0.59	-0.01
25	-0.57	-0.56	-0.01
26	-0.56	-0.58	+0.02
27	-0.55	-0.56	+0.01
28	-0.60	-0.65	+0.05
29	-0.46	-0.45	-0.01
30	-0.62	-0.63	+0.01
31	-0.56	-0.59	+0.03
32	-0.59	-0.63	+0.04
33	-0.56	-0.54	-0.02
34	-0.71	-0.65	-0.06
35	-0.66	-0.63	-0.03
36	-0.68	-0.69	+0.01

Table-2: Data from PLS Cross-validated analysis (For Test Set)

Compound	Actual log (BA)	Calculated log (BA)	Residual
01	-0.70	-0.73	+0.03
02	-0.51	-0.48	-0.03
03	-0.56	-0.55	-0.01
04	-0.61	-0.53	-0.08
05	-0.62	-0.63	+0.01
06	-0.54	-0.60	+0.06

The results of the CoMFA studies are summarized in **Table-3**. From this table it is evident that the CoMFA derived QSAR shows a good cross validated r^2, (0.714) and conventional r^2, 0.889, therefore indicates a considerable predictive and correlative capacity of the model. In this analysis both steric and electrostatic field contribute to the QSAR equation by 83.3% and 16.7%, respectively, suggesting that variation in biological activity of compounds is dominated by differences in steric (van der Waals) interactions.

The real test for model predictiveness is to predict the activity of ligands, which were not used in the model generation. Test set has 06 ligands or compounds, which were randomly kept aside as a test set. The CoMFA models exhibited a good predictiveness on these ligands (Table-4).

To visualize the CoMFA steric and electrostatic fields from PLS analysis, contour maps of the product of the standard deviation associated with the CoMFA column and coefficient (SD X coeff.) at each lattice point were generated. The contour maps are plotted as percentage contribution to the QSAR equation and are associated with the differences in biological activity.

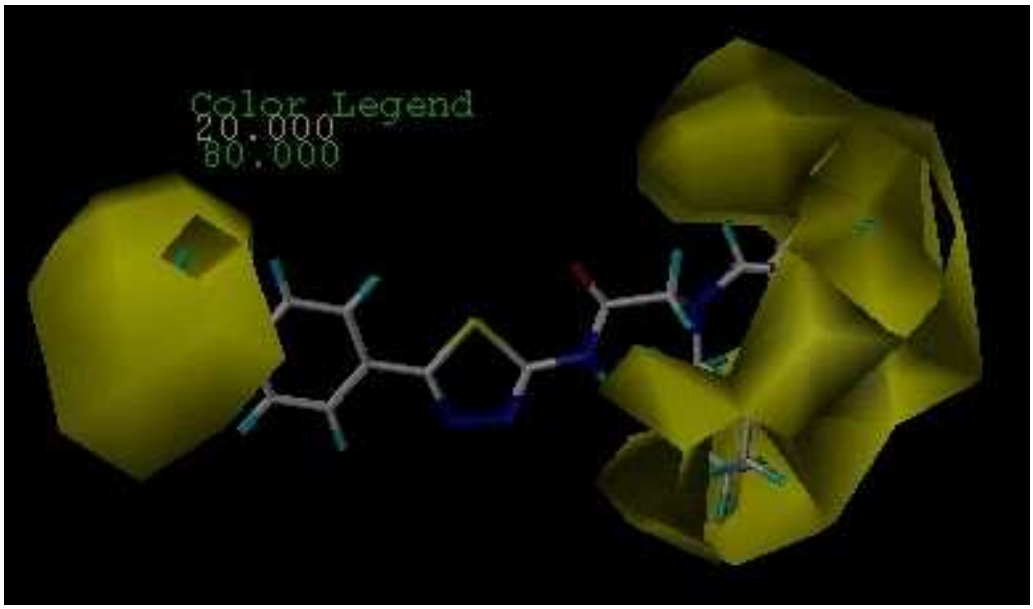

Figure-2a: Steric contour plot: favored (contribution level 80%) and unfavored (contribution level 20%) areas are represented as green and yellow contours, respectively.

In **Figure-2a** the regions of high and low steric tolerance are shown in green and yellow polyhedral, respectively. The areas of high bulk tolerance (80% contribution) are observed near P1 and P3 positions of the ligands (Figure-1). The active analogue (Compound 20) shown in Figure-2a, shows that cyclohexyl ring embedded in the green region at P1 site. The spontaneous motor activity shown by the compounds 29, 23, 22, 12, 11, 3, 9 and 13 etc., was due to the presence of bulky groups in P1 position surrounded by green contours in the steric field plot.

In the present sterically unfavored yellow regions were observed near the P1 and P3 position. The steric bulk in this region has a negative effect on the activity as represented by low activity of the compounds 10, 4, 2, 19, 34, 6, 21

etc. Sterically unfavored yellow contours are also present at P2 position, embedded in the surrounding green contours, suggesting that there is a definite requirement of a substructure with appropriate shape to exhibit high activity.

CoMFA electrostatic fields are shown as blue and red polyhedral in **Figure- 2b**. A low electron density within the molecules near blue and red polyhedral, respectively, increases or decreases the activity and vice versa. Presence of a blue contour at P1 and P3 position suggesting that a low electron density in this area will have a positive effect on the biological activity (compounds 20, 29, 23, 22, 3 etc.) and substructures with high electron density will reduce the activity (compounds 10, 4, 15, 8, 2 etc.). Presence of red contours at P3 position suggest that high electron density in this region increases the activity (compounds 11, 12, 16, 17, 18 etc.).
Though the electrostatic field contributions are less, a small change in electrostatic interactions will have a considerable effect on the activity.

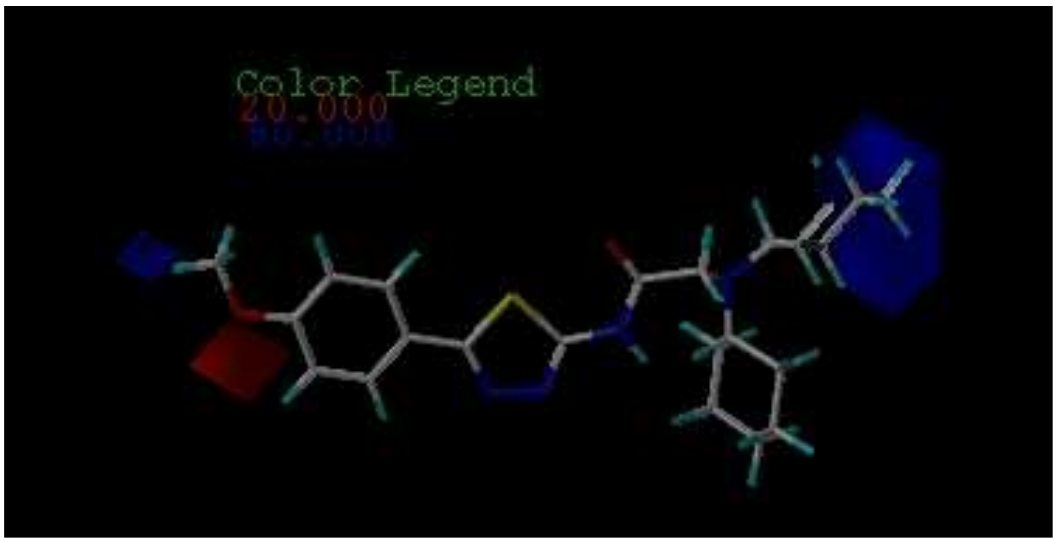

Figure-2b: Electrostatic contour plot: positive (contribution level of 80%) and negative (contribution level of 20%) charge favoring areas are represented as blue and red contours, respectively.

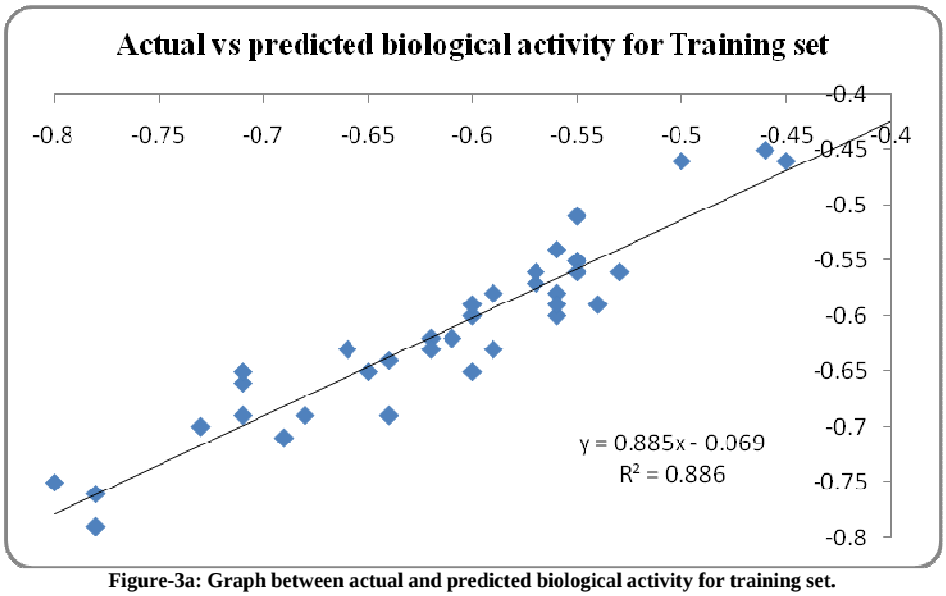

Figure-3a: Graph between actual and predicted biological activity for training set.

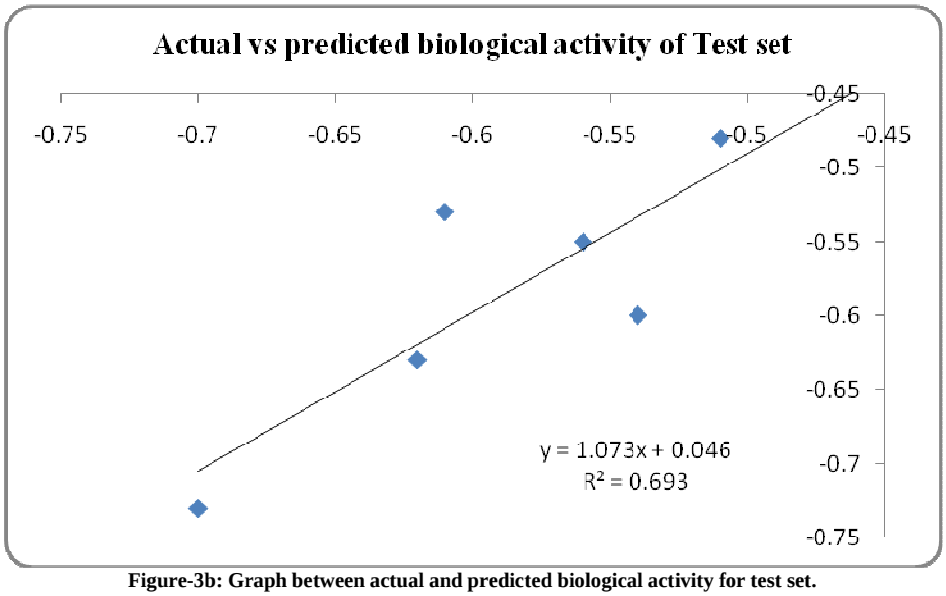

Figure-3b: Graph between actual and predicted biological activity for test set.

The observed vs. predicted activity provides an idea about how well the model was trained and how well it predicts the activity of the external test set. From the plot (Figure 3a and 3b) it can be seen that model is able to predict the activity of training set quite well (all points are close to the regression line) as well as external test set providing confidence in the predictive ability of the model.

Acknowledgement
We are thankful to the Head, Department of Pharmaceutical Sciences, Dr. H. S. Gour University, Sagar (MP) and Molecular Modeling Division, IICT, Hyderabad (AP) for their help. SKJ is thankful to UGC, New Delhi for the award of JRF during his PhD.

REFERENCES

[1] R. D. Cramer, D. E. Patterson, J. D. Bunce, *J. Am. Chem. Soc.*, **1988**, 110, 5959-5967.
[2] M. Clark, R. D. Cramer, D. M. Jones, D. E. Patterson, P. E. Simeroth, *Tetrahedron Comput. Methodology*, **1990**, 3, 47-59.
[3] P. S. Charifson (ed): "Practical Application of Computer-Aided Drug Design", Marcel Dekker, Inc., New York, **1997**.
[4] S. S. Kulkarni, L. K. Gediya, V.M. Kulkarni, *Bioorg. Med. Chem.*, **1999**, 7, 1475.
[5] S. S. Kulkarni, V. M. Kulkarni, *J. Med. Chem.*, **1999**, 42, 373.
[6] M. L. Brown, C. C.Zha, C. C. Van Dyke, G. B. Brown, W. J. Brouillette, *J. Med. Chem.*, **1999**, 42, 1537.
[7] C. T. Supuran, *Nat. Rev. Drug Discov.*, **2008**, 7, 168-181.
[8] M. Bülbül, N. Saraço glu, Ö._I. Küfrevio_glu, M. Çiftçi, *Bioorg. Med. Chem.*, **2002**, 10, 2561-2567.
[9] M. Bülbül, R. Kasımo_gulları, Ö._I. Küfrevio_glu, *J. Enz. Inhib. Med. Chem.*, **2008**, 23, 895-900.
[10] C. T. Supuran, F. Mincione, A. Scozzafava, F. Briganti, G. Mincione, M. A. Ilies, *Eur. J. Med. Chem.*, **1998**, 33, 247-254.
[11] V. K. Agrawal, M. Banerji, M. Gupta, J. Singh, P. V. Khadikar, C. T. Supuran, *Eur. J. Med. Chem.*, **2005**, **40**, 1002-1012.
[12] A. Thiry, A. Delayen, L. Goossens, R. Houssin, M. Ledecq, A. Frankart, J.-M. Dogne, J. Wouters, C.T. Supuran, J.-P. Hénichart, B. Masereel, *Eur. J. Med. Chem.*, **2009**, 44, 511-518.
[13] J. Y. Winum, A. Thiry, K. E. Cheikh, J. M. Dogné, J. L. Montero, D. Vullo, A. Scozzafava, B. Masereel, C. T. Supuran, *Bioorg. Med. Chem. Lett.*, **2007**, 17, 2685-2691.
[14] J. S. Schuman, *Clin. Therap.*, **2000**, 22, 167-208.
[15] M. A. Santos, S. Marques, D. Vullo, A. Innocenti, A. Scozzafava, C. T. Supuran, *Bioorg. Med. Chem. Lett.*, **2007**, 17, 1538-1543.
[16] F. A. Ashour, N. S. Habib, M. Taibbi, S. Dine, A. Dine, *Farmaco*, **1990**, 45, 1341-1349.

[17] K. Parmar, S. Prajapati, R. Patel, R. Patel, *Res J Chem Sci.*, **2011**, 1, 18-24.
[18] P.-F. Xu, Z.-H. Zheng, X.-P. Hui., *J. Chinese Chem. Soc.*, **2004**, 51, 315-319.
[19] O. Pintilie, L. Profire, V. Sunel, M. Popa, A. Pui, *Molecules*, **2007**, 12, 103-13.
[20] H. Rajak, R. Veerasamy, A. K. Gupta, M. D. Kharya, P. Mishra, *Digest J. Nanomaterials Biostructures*, **2009**, 4 (3), 443-51.
[21] E. Akbas, I. Berber, *Eur. J. Med. Chem.*, **2005**, 40, 401-405.
[22] J. Tao, D.-Z. Wang and L.-H. Cao, *J Chinese Chem Soc.*, **2010**, 57, 1077-80.
[23] M. M. Burbuliene, V. Sakociute, P. Vanilavicius, *ARKIVOC*, **2009**, xii, 281-89.
[24] S. Joshi, A. D. Manikpuri, D. Khare, *J. Indian Chem. Soc.*, **2008**, 85, 508–512.
[25] M. Ciotti, S. Humphreys, J. Venditti, N. Kaplan, A. Goldin, *Am. Asso. Can. Res.*, **2011**, 2, 1195-1201.
[26] S. Karakus, U. Coruh, B. B.-D. Ezequiel M. V.-Lopez, S. O.-Turan, J. Akbuga, S. Rollas, *Marmara Pharm J.*, **2010**, 14, 84-90.
[27] A. Foroumadi, Z. Kiani, F. Soltani, *IL Farmaco*, **2003**, 58, 1073-76.
[28] F. Hadizadeh, R. Vosooghi, *J Heterocyclic Chem.*, **2008**, 1, 45.
[29] A. K. Gadad, M. N. Noolvi, R. V. Karpoormath. *Bioorg. Med. Chem.*, **2004**, 12, 5651-59.
[30] A. W. Bauer, W. M. M. Kirby, J. C. Sherris, M. Turck, *Am. J. Clin. Pathol.*, **1966**, 45, 493.
[31] A. Foroumadi, M. Sorkhi, M. H. Moshafi, M. Safavi, A. Rineh, F. Siavoshi, A. Shafiee, S. Emami, *Med. Chem.*, **2009**, 5, 529-34.
[32] S. Giri, H. Singh, *J. Indian Chem. Soc.*, **1967**, 44, 145.
[33] V. S. Jamode, H. S. Chandak, P. R. Bhagat, *J. Indian Chem. Soc.*, **2008**, 85, 1169–1173.
[34] D. J. Haydon, I. Collins, L. G. Czapleurski, *PCT Int. Appl. WO. 37*, **2009**, 485.
[35] S. K. Jain, P. Mishra, *Indian J. Chem.*, **2004**, 43B, 184.
[36] S. K. Jain, *Ph.D. thesis*, Dr. H.S. Gour University (Sagar, India, 2001).
[37] S. K. Jain, P. Mishra, *Asian J. Chem.*, **2011**, 23 (3), 1305.
[38] W. W. Wilkerson, *Eur. J. Med. Chem.*, **1995**, 30, 191.
[39] R. D. Cramer, J. D. Bunce, D. E. Patterson, *Quant. Struct. Act. Relat.*, **1988**, 7, 18.